ICOSSAR '85
4th International Conference on Structural Safety and Reliability

Seismic Reliability Analysis of Underground Pipeline Network Systems

Masaru Kitaura[1], Fumio Yamazaki[2] and Masanobu Shinozuka[3]

[1] Dept. of Civil Engineering, Kanazawa University, Kanazawa, Japan
[2] Visiting Scholar, Columbia University; on leave from Shimizu Construction Co. Ltd., Tokyo, Japan
[3] Dept. of Civil Engineering and Engineering Mechanics, Columbia University, New York, NY, USA

ABSTRACT

The present study deals with the reliability or the probability of continued serviceability (connectivity) of urban telecommunications networks immediately after a major earthquake. A telecommunications network is idealized into a series system in parallel consisting of switching equipment (nodes) and trunk lines (links). First, all the possible tie-sets in the network are enumerated and the significant tie-sets are identified. Second, an analytical procedure is developed to evaluate the connectivity of the network, making use only of the significant tie-sets. In doing so, the randomness of the mode and link fragilities as well as of seismic loads is taken into consideration. Then, uncertainties in the fragility and seismic information are introduced by the Latin hypercube sampling method. Finally, the effects of these randomnesses and uncertainties are examined for a network model.

KEYWORDS

Telecommunication; network; reliability; earthquake; fragility; randomness; uncertainty; Latin hypercube sampling method.

1. INTRODUCTION

Under the NSF grant CEE-81-16842 entitled "Telecommunications Lifelines in a Seismic Environment," Columbia University and Weidlinger Associates developed a system network model for studying the reliability of urban telecommunications systems immediately after an earthquake and demonstrated how the model can be used for evaluating the seismic performance of telecommunications networks. While the model is probabilistic, the seismic performance of several key elements of the network, such as equipment fragility characteristics [1], were based, as much as possible, on a currently available physical understanding of element failure. Such elements comprise the nodes and links of the system network which are subjected to ground shaking. During the first phase of the project, the intensity of ground shaking was defined by peak accelerations and was related to the earthquake magnitude and epicentral distance by semi-emprical attenuation rules [2,3]. Local geology was taken into account by idealizing ground motions as vertically propagating SH waves by means of the shear beam approach. The physical nature and accuracy of the approximation introduced in such an idealization were examined in Ref. 4. Also, a network reliability analysis was performed by means of a modified version of a Monte Carlo simulation code (FAST) [5]. In Ref. 6, in order to focus our work on more critical issues of telecommunications facilities, we idealized a typical urban network of trunk lines (links) connecting central dial offices (nodes). Each district served by a Central Dial Office (CDO) corresponds roughly to a telephone prefix number and acts as a collection and distribution point for 10,000 to 100,000 users. Connections between individual users and their CDO were not considered at this stage.

Under the previous NSF grant (PFR-78-15049) entitled "Underground Lifelines in a Seismic Environment," probabilistic models and associated computer programs were developed to derive reliability estimates without recourse to Monte Carlo techniques for underground network systems, particularly for water transmission systems [7-10]. This paper summarizes how we modified these models and computer programs to be utilized for telecommunications systems without recourse to Monte Carlo techniques.

2. FRAGILITIES OF NODES AND LINKS

In Ref. 1, the damage modes for facilities and equipment typically found in Central Dial Offices under earthquakes were surveyed. A modal analysis was performed using input response spectra from several different real earthquake records. Conservative estimates for thresholds of the spectral acceleration required to cause damage and to cause collapse were found to be approximately 0.6g and 1.0g respectively.

Based on this previous research, we assumed the resisting capacity α_R of nodes to be a random variable whose distribution function (fragility curve) is depicted in Fig. 1. In the present study, the fragility curve is given by a Gaussian distribution function with specified mean value $\bar{\alpha}_R$ and coefficient of variation $COV(\alpha_R)$. In order to introduce uncertainty into the fragility information, it is further assumed that the mean value $\bar{\alpha}_R$ can be interpreted as a random variable governed by a beta (β) distribution while $COV(\alpha_R)$ does not involve any uncertainty and therefore is constant. Hence, the fragility of a node with respect to the response acceleration is given by a family of Gaussian distribution functions as also depicted in Fig. 1 with $\bar{\alpha}_R$, $\bar{\bar{\alpha}}_R$ and $\underline{\alpha}_R$ indicating the mean value, upper and lower bounds of $\bar{\alpha}_R$, respectively.

Similarly, the fragility curve for a link is assumed to be given by a Gaussian distribution function with mean value $\bar{\varepsilon}_R$ and coefficient of variation $COV(\varepsilon_R)$ under the assumption that network links are strain-sensitive. As in the case of a node, uncertainty in the fragility information is reflected by the assumption that $\bar{\varepsilon}_R$ can be interpreted as a random variable, again governed by a beta distribution, while $COV(\varepsilon_R)$ is constant. Thus, the fragility of a link is also represented by a family of Gaussian distribution functions as shown in Fig. 2 with $\bar{\varepsilon}_R$, $\bar{\bar{\varepsilon}}_R$ and $\underline{\varepsilon}_R$ indicating the mean value, upper and lower bounds of $\bar{\varepsilon}_R$, respectively.

In general, the beta distribution function of a random variable

X $(x^- < X < x^+)$ has a density function $f_X(x)$ given by

$$f_X(x) = \frac{1}{(x^+ - x^-)} \frac{\Gamma(\gamma + \eta)}{\Gamma(\gamma)\Gamma(\eta)} \left(\frac{x - x^-}{x^+ - x^-}\right)^{\gamma-1} \left(1 - \frac{x - x^-}{x^+ - x^-}\right)^{\eta-1} \tag{1}$$

where $\Gamma(\cdot)$ is the gamma function, γ and η are parameters of the distribution with mean value $E\{X\}$ and variance $Var\{X\}$ given by

$$E\{X\} = x^- + \frac{\gamma}{\eta+\gamma}\left(x^+ - x^-\right), \quad Var\{X\} = \frac{\eta\gamma}{(\eta+\gamma)^2(\eta+\gamma+1)}\left(x^+ - x^-\right)^2 \tag{2}$$

In the present study, $\gamma = \eta = 2$ is assumed.

It is recognized that the fragility curves for links depend on, among other things, the length of their lengths. While the present study disregards this issue, Refs. 7, 8 and 13 addressed it from different points of view. No conclusive consensus appears to be available with respect to this at the present, however.

3. EARTHQUAKE RESPONSES OF NODES AND LINKS

The Esteva model for attenuation is used here as in Refs. 7-9. The model relates the Richter magnitude M and focal distance R (km) to the peak ground acceleration α (cm/sec^2),

$$\alpha = \frac{5600\ \exp(0.8M)}{(R + 40)^2}, \qquad R > 15\ \text{km}, \tag{3}$$

Using the above expression for acceleration, we can determine, in approximation, the Modified Mercalli Intensity I [11] in terms of M and R;

$$I = 3\left(\log_{10}\alpha + 0.5\right) \tag{4}$$

and then evaluate the maximum free-field velocity V [12] in terms of M and R;

$$V = 0.3 \times 10^{0.18I} \qquad (\text{cm/sec}) \tag{5}$$

The reason for this procedure is to obtain the free-field ground strain, which is to be used as an environmental input to the network. Also, as in Refs. 7-9, the ground strain spectrum $\varepsilon(\omega)$ is obtained as

$$\varepsilon(\omega) = S_V(\omega)/c(\omega) \simeq V/c \tag{6}$$

where $S_V(\omega)$ is the velocity spectrum and $c(\omega)$ is the phase velocity of the seismic wave as a function of frequency. The third member of Eq. 6 is derived by observing that the phase velocities near the ground surface are approximately constant for specific soil conditions, i.e., $c(\omega) = c$ and that $S_V(\omega)$ is conservatively approximated by V in Eq. 5. Based on the above observation, the ground strain spectrum $\varepsilon(\omega)$ is simply written as ε and given by the third member of Eq. 6.

The response acceleration α_L of a node and the response strain ε_L of a link are respectively given by

$$\alpha_L = TF_\alpha \times \alpha, \quad \varepsilon_L = TF_\varepsilon \times \varepsilon \tag{7}$$

where TF_α and TF_ε represent the response amplification factors. In the present study, c is assumed to be 266 m/sec, TF_α is taken as 3.0 for all the nodes and TF_ε as 2.0 for all the links.

Under deterministic seismic loading conditions, the earthquake responses of a node and a link are evaluated by Eq. 7 for assumed values of M and R. It appears rather difficult to properly evaluate the randomness and uncertainty of the seismic response of the ground given by Eqs. 3 and 6. We introduce, however, randomness and uncertainty into the response in the same manner as we did for the fragilities. Hence, the response curve of a node is given by a Gaussian distribution function with mean value $\bar{\alpha}_L$ and coefficient of variation $COV(\alpha_L)$ as depicted in Fig. 3. Uncertainty in the response acceleration is reflected by the assumption that $\bar{\alpha}_L$ can be interpreted as a random variable governed by the beta distribution, while $COV(\alpha_L)$ is constant. This gives rise to a family of Gaussian distribution functions for α_L as also shown in Fig. 3 where $\bar{\bar{\alpha}}_L$, $\bar{\alpha}_L^+$ and $\bar{\alpha}_L^-$ indicate the mean value, upper and lower bounds of $\bar{\alpha}_L$, respectively. The response strain ε_L of a link is also represented by a family of Gaussian distribution funcfunctions as shown in Fig. 4 with $\bar{\bar{\varepsilon}}_L$, $\bar{\varepsilon}_L^+$ and $\bar{\varepsilon}_L^-$ indicating the mean value, upper and lower bounds of $\bar{\varepsilon}_L$, respectively. By virtue of the first-order second-moment method, the value of ε corresponding to α by way of Eqs. 3, 4, 5 and 6 represents the mean value of ε in approximation and the coefficient of variation of ε is calculated as follows.

$$COV(\varepsilon_L) = 0.54COV(\alpha_L) \tag{8}$$

In the present study, the random variables α_L and ε_L at individual nodes and links are assumed to be independent. In fact, this assumption is consistent with the way in which the serviceability probability of the network is evaluated with the aid of Eqs. 9-10. However, this assumption is not particularly realistic if we realize that α_L and ε_L represent "common cause" efforts of the earthquake; α_L and ε_L at individual nodes and links are supposedly completely dependent or at least highly correlated. The reality probably lies between the values obtained under the assumptions of total independence (as assumed in the present study) and complete dependence. The random variables α_R and ε_R for individual nodes and links may also be highly correlated.

4. RELIABILITY ANALYSIS OF NETWORK SYSTEMS

Figure 5 depicts the idealized telecommunications network model used in Ref. 6. Trunk lines representing anywhere from 20,000 to 60,000 connections provide links between Central Dial Offices (nodes). The site has been assumed to be about 50 km from the focus (assumed to be the same as the epicenter in approximation) and of characteristic dimension 15 km. Different epicentral distances for each node and link have been incorporated into the calculation.

A computer code was developed to enumerate all the tie-sets between an arbitrary two nodes of the network on the basis of a node connection matrix. This route-finding procedure is illustrated by a flow chart in Fig. 6.

The analytical procedure for calculating the serviceability of a network system was discussed in Ref. 13. In general, a network of series systems in parallel (SSP) consists of NT component tie-sets (series system); TS_1, TS_2, ..., TS_K, ..., TS_{NT} with the k-th tie-set, TS_K, consisting of NL_k elements, where an element means a node or a link. Taleb-Agha [14,15] formulated the method of evaluating the probability of failure of such an SSP system. In particular, the probability P_S(any p/NT) that any p of the NT tie-sets in the SSP system would survive was given by

$$P_s(\text{any } p/NT) = \sum_{i=1}^{NT} K_{pi} \sum_{j=1}^{NC_i} T_{ji} \qquad (9)$$

where $NC_i = \binom{NT}{i}$; $K_{pi} = K_{(p-1)(i-1)} - K_{p(i-1)}$ in the case of $1 < p \leq i$; $K_{pi} = 0$ in the case of $p > i$ and $K_{1i} = (-1)^{i-1}$.

Obviously, except for very simple networks, some of these tie-sets share some elements and hence they are usually dependent. Then, the quantity T_{ji} in Eq. 9 is given by

$$T_{ji} = \prod_{L_n \varepsilon US_j^i} P_s(L_n) \quad \text{with} \quad US_j^i = \bigcup_{k\varepsilon I_j^i} TS_k \qquad (10)$$

where U denoted the union as usual, and L_n identifies the n-th element in the set of all elements in the entire system which consists of $\sum_{k=1}^{NT} NL_k$ elements. Since I_j^i is a set of positive integers defining the tie-set combination taken i tie-sets out of NT tie-sets at a time, T_{ji} is the probability that all the tie sets out of that combination will survive. The survival probability of the element P_s in Eq. 10 is defined by

$$P_s = 1 - P\{\alpha_R < \alpha_L\} \ , \ P_s = 1 - P\{\varepsilon_R < \varepsilon_L\} \qquad (11)$$

for nodes and links, respectively.

The procedure for the reliability analysis of network systems is shown in Fig. 7. For the first step, assuming that all the tie-sets are independent, we can evaluate the probability of survival of each tie-set without difficulty. For this evaluation, the best estimate distribution functions with mean values $\bar{\bar{\alpha}}_R$, $\bar{\bar{\varepsilon}}_R$, $\bar{\bar{\alpha}}_L$, $\bar{\bar{\varepsilon}}_L$ (mean values of $\bar{\alpha}_R$, $\bar{\varepsilon}_R$, $\bar{\alpha}_L$, $\bar{\varepsilon}_L$) are used; recall that $\bar{\alpha}_R$, etc. are random variables with beta distribution functions. Identifying only those significant tie-sets for which the survival probabilities are sufficiently high, and performing a rigorous probabilistic analysis on a parallel system consisting of only these tie-sets, we can obtain the probability of survival between these two nodes in a very good approximation. The Latin hypercube sampling method is also incorporated in this phase of the analysis in order to take into account the uncertainties in the fragility information and seismic response of the network system.

5. NUMERICAL EXAMPLE

The survival (connectivity) between nodes 7 and 1 of the network system shown in Fig. 5 is considered. All the possible tie-sets (43 of them) are enumerated in Fig. 8. Under various earthquake magnitudes (M = 6.0, 6.1, ..., 7.2), two cases of seismic loading conditions are considered. (1) Random loading conditions: α_L and ε_L are assumed to be Gaussian random variables whose mean values are computed from Eq. 7. Their coefficients of variation are assumed to be $COV(\alpha_L) = 0.200$ and $COV(\varepsilon_L) = 0.108$; (2) Random and uncertain loading conditions: the upper and lower bounds of the beta distributions are assumed to be

$$\bar{\alpha}_L^{\pm} = (1.0 \pm 0.447)\bar{\bar{\alpha}}_L \quad \text{and} \quad \bar{\varepsilon}_L^{\pm} = (1.0 \pm 0.241)\bar{\bar{\varepsilon}}_L$$

whereas randomness and uncertainty are always considered in the fragility characteristics of the nodes and links as shown in Figs. 1 and 2.

Assuming independence of each tie-set, eight significant tie-sets (those with asterisks in Fig. 8) are chosen. The probability of failure at all the nodes and links are then computed for twenty-four fragility curves corresponding to the twenty-four values of $\bar{\alpha}_R^{(i)}$ and $\bar{\varepsilon}_R^{(i)}$ (i=1,2,...,24) such that

$$P\{\bar{\alpha}_R < \bar{\alpha}_R^{(i)}\} = (2i-1)/48 \quad \text{and} \quad P\{\bar{\varepsilon}_R < \bar{\varepsilon}_R^{(i)}\} = (2i-1)/48.$$

Generating twenty-four sample network systems by means of the Latin hypercube sampling method, we obtain, for each earthquake magnitude considered, twenty-four values of the failure probability P_f that connectivity between nodes 7 and 1 will be lost. The results are plotted in Fig. 9 for case 1. These results are replotted in Fig. 10 with confidence probability as a parameter. Similar results are plotted in Fig. 11 for case 2. For case 2, twenty-four acceleration and strain respnse curves are also incorporated in the same manner as done for the fragility information. Using the Latin hypercube sampling method for both the fragilities and responses, twenty-four values of the fail-probability of the system are also obtained. Comparison of Fig. 11 with Fig. 10 indicates that introducing uncertainty into the loading conditions makes the distribution ranges of P_f broader although the expected values of P_f are kept at similar values.

6. CONCLUSION

In the analysis described above, we (a) developed a computer program which can automatically enumerate all the tie-sets between any two nodes of a network; (b) evaluated analytically the probability of serviceability (connectivity) of a simplified telecommunications system taking into consideration the randomness of the node and link fragilities and their seismic responses; (c) incorporated the Latin hypercube sampling technique to estimate the systematic uncertainty in the fragility and seismic load information; and (d) examined the effects of randomness and uncertainty in the seismic load on the probability of serviceability.

7. ACKNOWLEDGEMENT

This work was done under NSF Grant No. CEE-81-16842 with Dr. K. Thirumalai as Program Director.

REFERENCES

(1) ISENBERG, J., "Seismic Analysis of Telecommunications Equipment-Building Systems," Proceedings of the 4th ASME Pressure Vessel and Piping Conference, Portland, Oregon, June 1983.

(2) SHINOZUKA, M. and BENAROYA, H., "Seismic Reliability of Telecommunications Networks," Proceedings of the 4th ASME Pressure Vessel and Piping Conference, Portland, Oregon, June 1983.

(3) SHINOZUKA, M., ISENBERG, J. and BENAROYA, H., "Telecommunications Lifelines in a Seismic Environment," Proceedings of the 8th World Conference on Earthquake Engineering, San Francisco, California, July 1984.

(4) SHINOZUKA, M., KAMEDA, H. and KOIKE, T., "Ground Strain Estimation for Seismic Risk Analysis of Underground Lifelines," Journal of the Engineering Mechanics Division, ASCE, Vol. 109, No. 1, February 1983, pp. 175-191.

(5) TRW SYSTEMS GROUP, "Failure Analysis by Statistical Techniques (FAST), Volume 1, User's Manual," DNA 3336F-1, October 31, 1974.

(6) BENAROYA, H., SHINOZUKA, M. and KITAURA, M., "Reliability of Telecommunications Networks," Technical Report No. 3 under NSF Grant No. CEE-81-16842, December 1983.

(7) SHINOZUKA, M., TAKADA, S. and ISHIKAWA, H., "Some Aspects of Seismic Risk Analysis of Underground Lifeline Systems," Journal of Pressure Vessel Technology, ASME, Vol. 101, February 1979, pp. 31-43.

(8) SHINOZUKA, M. and KOIKE, T., "Seismic Risk of Underground Lifeline Systems Resulting from Fault Movement," Proceedings of the 2nd US National Conference on Earthquake Engineering, Stanford, California, January 1979, pp. 663-672.

(9) SHINOZUKA, M., TAN, R. and KOIKE, T., "Serviceability of Water Transmission Systems Under Seismic Risk," Proceedings of the ASCE Specialty Conference on Lifeline Earthquake Engineering, Oakland, California, August 20-21, 1981, pp. 97-110.

(10) TAN, R. and SHINOZUKA, M., "Optimization of Underground Water Transmission Network Systems Under Seismic Risk," Journal of Soil Dynamics and Earthquake Engineering, Vol. 1, No. 1, 1983, pp. 30-38.

(11) GUTENBERG, B. and RICHTER, C.F., "Earthquake Magnitude, Intensity, Energy and Acceleration," Bulletin of the Seismological Society of America, Vol. 32, 1942, pp. 163-191.

(12) KANAI, K., Seismological Engineering, (Tokyo: Kyoritsu Press), 1973.

(13) SHINOZUKA, M., TAKADA, S. and KAWAKAMI, H., "Risk Analysis of Underground Lifeline Network Systems," Proceedings of the US-Southeast Asia Symposium on Engineering for Natural Hazards Protection, University of Illinois at Urbana-Champaign, 1978, pp. 44-58.

(14) TALEB-AGHA, G., "Seismic Risk Analysis of Networks," Seismic Design Decision Analysis - Report No. 22, Dept. of Civil Engineering, MIT, Research Report R75-43, November 1975.

(15) TALEB-AGHA, G., "Seismic Risk Analysis of Lifeline Networks," Seismic Design Decision Analysis - Report No. 24, Dept. of Civil Engineering, MIT, Research Report R75-49, December 1975.

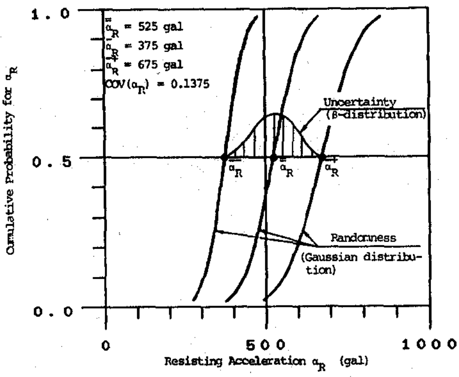

Fig. 1 Fragility Curves for Nodes

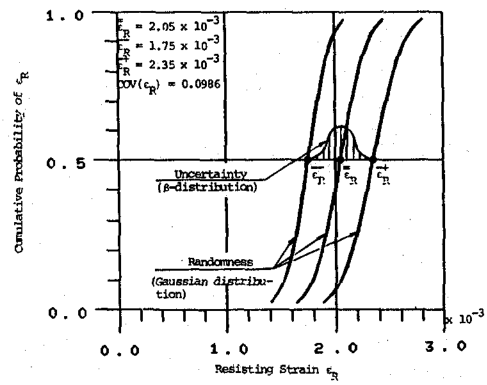

Fig. 2 Fragility Curves for Links

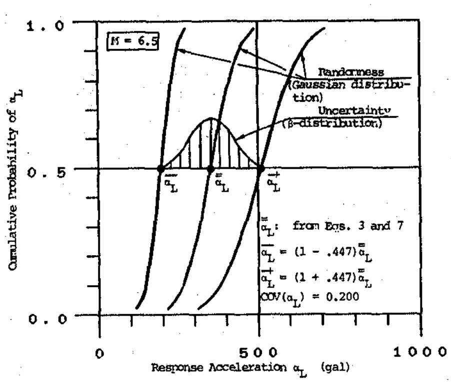

Fig. 3 Response Acceleration at Node 1

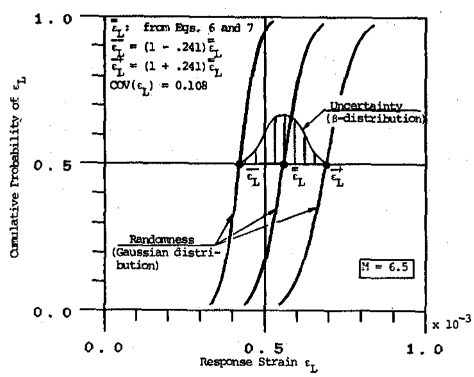

Fig. 4 Response Strain for Link 1

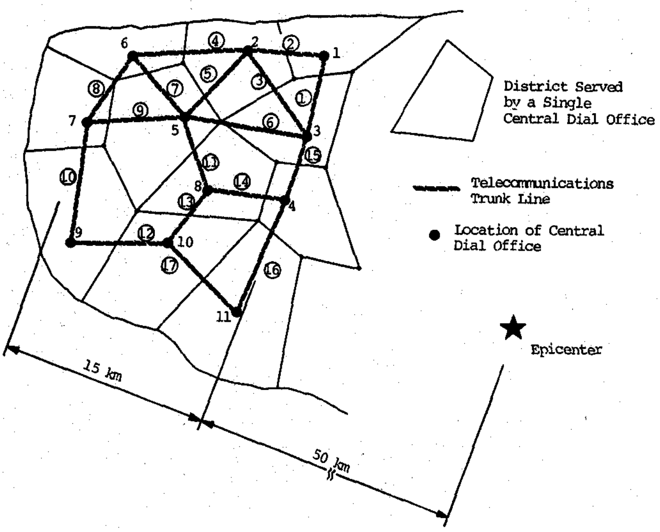

Link #	Number of Lines/10,000
1	4
2	4
3	3
4	3
5	2
6	4
7	2
8	6
9	4
10	5
11	3
12	3
13	2
14	3
15	3
16	6
17	5

Link numbers are circled, node numbers are not

Fig. 5 Plan View of An Idealized Telecommunications Network

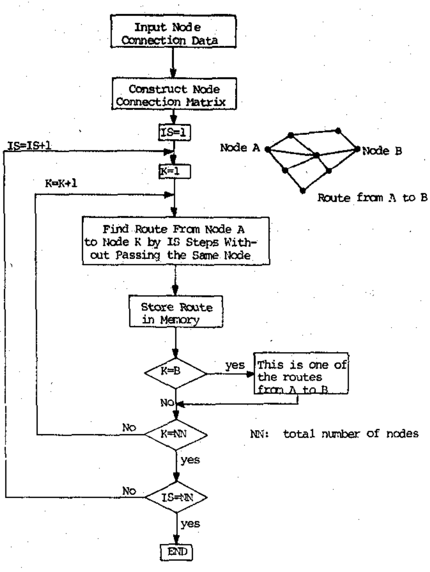

Fig. 6 Procedure to Find Route Between Nodal Points

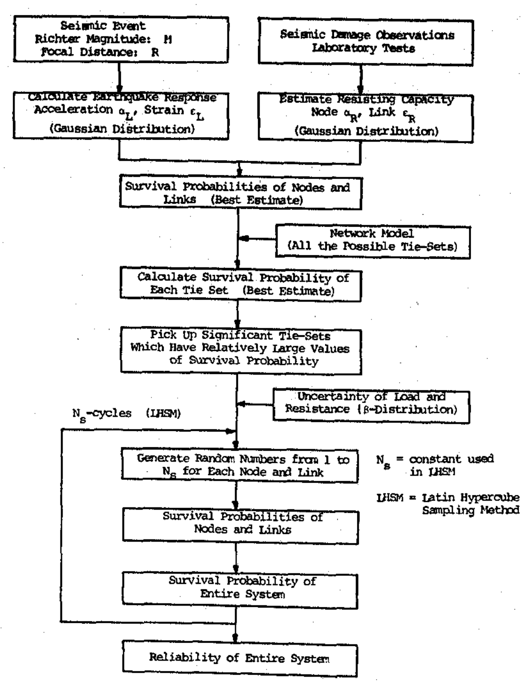

Fig. 7 Flow Chart of Reliability Analysis for a Telecommunications Network

Tie-Set No	# Steps	Nodal Paths
* 1	4	7 5 2 1
* 2	4	7 5 3 1
* 3	4	7 6 2 1
4	5	7 5 2 3 1
5	5	7 5 3 2 1
* 6	5	7 5 6 2 1
7	5	7 6 2 3 1
* 8	5	7 6 5 2 1
* 9	5	7 6 5 3 1
10	6	7 5 6 2 3 1
11	6	7 5 8 4 3 1
12	6	7 6 2 5 3 1
13	6	7 6 5 2 3 1
14	6	7 6 5 3 2 1
15	7	7 5 8 4 3 2 1
16	7	7 6 5 8 4 3 1
17	7	7 9 10 8 4 3 1
*18	7	7 9 10 8 5 2 1
19	7	7 9 10 8 5 3 1
20	7	7 9 10 11 4 3 1
21	8	7 5 8 10 11 4 3 1
22	8	7 6 2 5 8 4 3 1
23	8	7 6 5 8 4 3 2 1
24	8	7 9 10 8 4 3 2 1
25	8	7 9 10 8 5 2 3 1
26	8	7 9 10 8 5 3 2 1
*27	8	7 9 10 8 5 6 2 1
28	8	7 9 10 11 4 3 2 1
29	9	7 5 8 10 11 4 3 2 1
30	9	7 6 5 8 10 11 4 3 1
31	9	7 9 10 8 4 3 5 2 1
32	9	7 9 10 8 5 6 2 3 1
33	9	7 9 10 11 4 3 5 2 1
34	9	7 9 10 11 4 8 5 2 1
35	9	7 9 10 11 4 8 5 3 1
36	10	7 6 2 5 8 10 11 4 3 1
37	10	7 6 5 8 10 11 4 3 2 1
38	10	7 9 10 8 4 3 5 6 2 1
39	10	7 9 10 11 4 3 5 6 2 1
40	10	7 9 10 11 4 8 5 2 3 1
41	10	7 9 10 11 4 8 5 3 2 1
42	10	7 9 10 11 4 8 5 6 2 1
43	11	7 9 10 11 4 8 5 6 2 3 1

* Significant Tie-Sets

Fig. 8 Nodal Paths Between Nodes 7 and 1

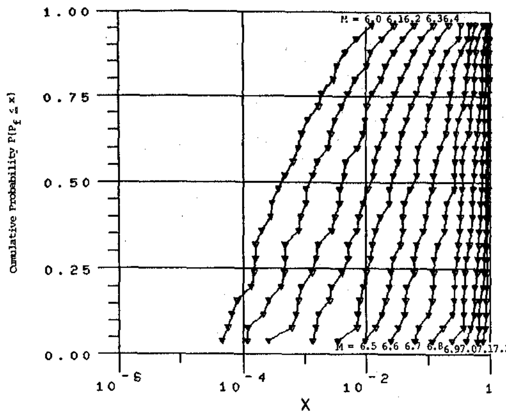

Fig. 9 Cumulative Probability of P_f for the Entire System (Under Random Loading Conditions)

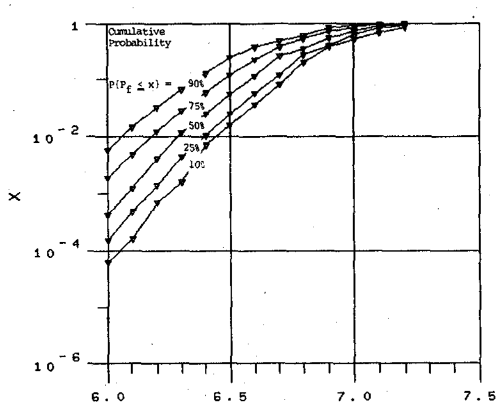

Fig. 10 Relationship Between Richter Magnitude M and P_f for the Entire System at Different Confidence Values (Under Random Loading Conditions)

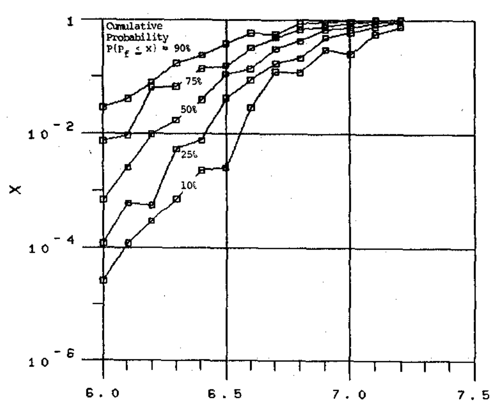

Fig. 11 Relationship Between Richter Magnitude M and P_f for the Entire System at Different Confidence Values (Under Random and Uncertain Loading Conditions)